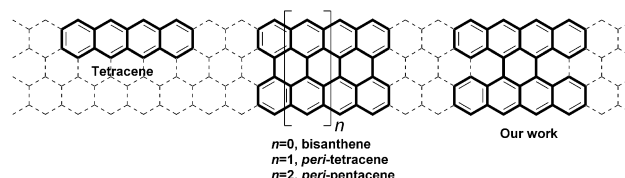


# Tetrabenzo[a,f,j,o]perylene: A Polycyclic Aromatic Hydrocarbon With An Open-Shell Singlet Biradical Ground State\*\*

Junzhi Liu, Prince Ravat, Manfred Wagner, Martin Baumgarten, Xinliang Feng,\* and Klaus Müllen\*

**Abstract:** A novel tetrabenzo[a,f,j,o]perylene, namely “bistetracene” in which two tetracenes are connected side by side with two bonds, was synthesized and characterized. An optical energy gap of about 1.56 eV is derived from the UV/Vis absorption spectrum, showing the low optical gap feature of such zigzag-edged polycyclic aromatic hydrocarbons (PAHs). Theoretical calculations and physical property investigations manifest that such a PAH possesses a prominent biradical character in the ground state, which is the first example among bistetracene derivatives. However, the bistetracene can easily undergo oxidation to tetrabenzo[a,f,j,o]perylene-9,19-dione (diketone) under ambient conditions. Thereby, such zigzag-edged PAH provides insight into understanding the edge state of other expanded homologues, such as *peri*-tetracenes or *peri*-pentacenes.

**P**olyacenes display fascinating electronic and optoelectronic properties resulting from the spin-polarized state at the zigzag edges.<sup>[1]</sup> To date, a number of reports have been published on organic field-effect transistors (OFETs) or organic light-emitting diodes (OLEDs) that use tetracene, pentacene, and their derivatives.<sup>[2]</sup> However, the longer acenes, such as hexacene, and higher homologues, are susceptible to oxidation under ambient conditions and photolytic degradation, which causes difficulties in their synthesis.<sup>[3]</sup> On our way to pursue the synthesis of *peri*-fused acene molecules (Scheme 1), which represent a series of conjugated systems with two rows of acenes *peri*-fused together, we must meet similar challenges. Theoretical calculations predict that the energy gap drastically decreases upon increasing the length of



**Scheme 1.** Structure of typical *peri*-fused acenes.

the *peri*-fused acenes.<sup>[4]</sup> The synthesis of higher homologous, such as *peri*-tetracene (Scheme 1), is expected to face low solubility, a small energy gap and high reactivity under ambient condition.<sup>[5]</sup> The smaller analogues, perylene and bisanthrene, have been known for a long time. However, the attempts to synthesize the next generation of *peri*-fused acenes, namely *peri*-tetracene, have not been successful yet, probably due to the extremely high reactivity as well as the lack of proper synthetic protocols.<sup>[6]</sup>

Recently, polycyclic aromatic hydrocarbons (PAHs) with singlet biradical feature have been intensively explored.<sup>[7]</sup> Several representative types of stable open-shell PAHs have been reported, including bisphenalenyls,<sup>[8]</sup> indenofluorenes,<sup>[9]</sup> anthenes,<sup>[10]</sup> and zethrenes,<sup>[11]</sup> which allow a glimpse of their peculiar properties arising from the singlet biradical character. Theoretical and experimental results have demonstrated that the major driving force for a singlet biradical ground state is the gain of additional Clar sextet rings in the biradical resonance form in comparison to the closed-shell resonance form, as a result of gaining the aromatic stabilization energies.<sup>[11c,12]</sup> In this regard, the tetrabenzo[a,f,j,o]perylene (**TBP 1**), namely “bistetracene” in which two tetracenes are connected side by side with two bonds, has two aromatic sextets in the closed shell form and a maximum of five aromatic sextets in the biradical form (Figure 1), regardless of the positions of the radicals. From the resonance structures, we can see that the most reactive sites (C5 and C6) are located at zigzag edges within the two central benzene rings. To obtain stable and soluble materials, our design is to kinetically block the reactive sites with bulky mesityl groups (such as **1-1**). On the basis of the resonance structures, more aromatic sextets for the bistetracene **TBP 1-1** or **1-2** will help to stabilize the biradical resonance form, and thus it is expected to show more biradical character in the ground state.

In this work, we demonstrate the synthesis of **TBP 1**, which has a low optical energy gap and exhibits a singlet biradical character in the ground state<sup>[11c,e]</sup> (Scheme 2). First, selective Suzuki coupling between 1,4-dibromo-2,5-diiodobenzene (**2**) and commercially available *o*-tolylboronic acid gave the 2',5'-dibromo-2,2''-dimethyl-1,1':4',1''-terphenyl (**3**)

[\*] J. Liu, Dr. P. Ravat, Dr. M. Wagner, Prof. Dr. M. Baumgarten, Prof. Dr. K. Müllen  
Max Planck Institute for Polymer Research  
Ackermannweg 10, 55128 Mainz (Germany)  
E-mail: muellen@mpip-mainz.mpg.de

Prof. Dr. X. Feng  
Center for Advancing Electronics Dresden (cfaed) and  
Department of Chemistry and Food Chemistry  
Technische Universität Dresden  
01062 Dresden (Germany)  
E-mail: xinliang.feng@tu-dresden.de

[\*\*] This work was financially supported by ERC grants on NANOGRAPH, DFG Priority Program SPP 1459, EU Project GENIUS, UPGRADE, MoQuaS and EC under Graphene Flagship (No. CNECT-ICT-604391), and the Office of Naval Research BRC Program. We also acknowledge the help from Angelos Giannakopoulos and Prof. David Beljonne for the calculation.

Supporting information for this article is available on the WWW under <http://dx.doi.org/10.1002/anie.201502657>.

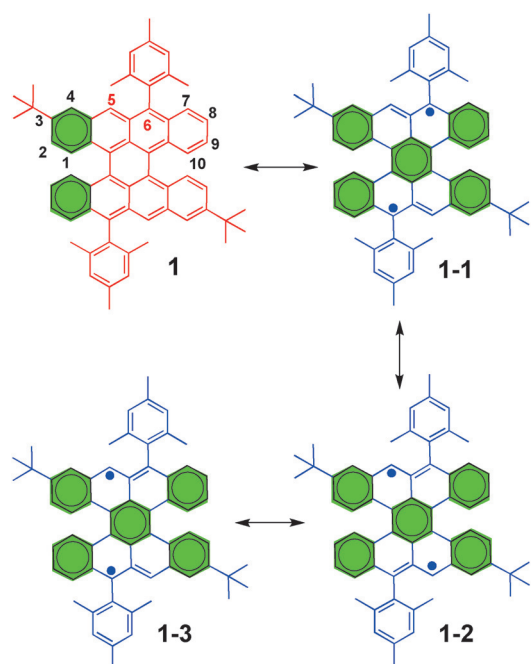
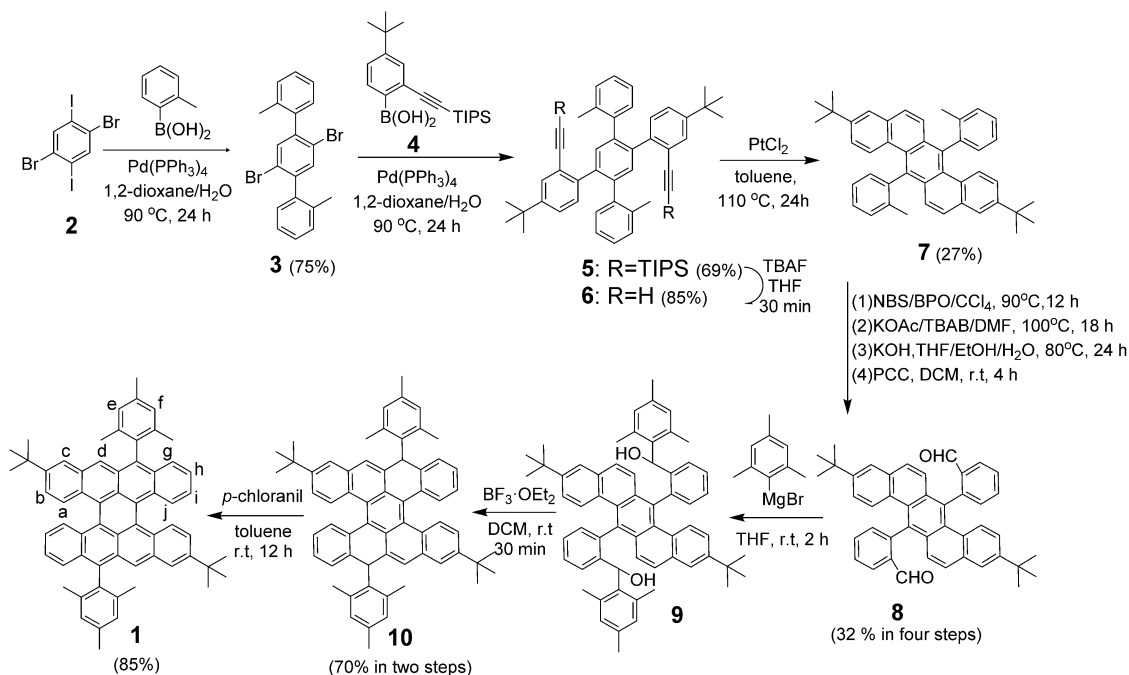


Figure 1. Resonance structures of **TBP 1**.

in 75 % yield. Then compound ((4,4''-di-*tert*-butyl-2',5'-di-*o*-tolyl-[1,1':4',1''-terphenyl]-2,2''-diyl)bis(ethyne-2,1-diyl))bis-(triisopropylsilane) (**5**) was prepared by Suzuki coupling of **3** with (4-(*tert*-butyl)-2-((triisopropylsilyl)ethynyl)phenyl)boronic acid (**4**) in 69 % yield. Desilylation of **5** under basic conditions afforded the diethynylterphenylene **6** in 85 % yield. Next, compound 3,10-di-*tert*-butyl-7,14-di-*o*-tolylbenzo[k]tetraphene (**7**) (for the crystal structure see Figure S4 in

the Supporting Information, SI) was obtained through the intramolecular cyclization of **6** in 27 % yield. The dimethyl groups of **7** were then transformed into dialdehyde functions to afford 2,2'-(3,10-di-*tert*-butylbenzo[k]tetraphene-7,14-diyl)dibenzaldehyde (**8**) through a bromination/esterification/hydrolysis/oxidation sequence in a yield of 32 %. Subsequently, compound **8** was treated with mesitylmagnesium bromide to give diol compound ((3,10-di-*tert*-butylbenzo[k]tetraphene-7,14-diyl)bis(2,1-phenylene))bis(mesitylmethanol) (**9**), which was subjected to Friedel–Crafts alkylation promoted by  $\text{BF}_3 \cdot \text{OEt}_2$  to afford 2,12-di-*tert*-butyl-9,19-dimesityl-9,19-dihydrotetrabenzo[a,f,j,o]perylene (**10**) in 70 % yield in two steps. Finally, the oxidation of **10** with *p*-chloranil in dry toluene at room temperature under argon afforded the target compound **TBP 1** as green powder in 85 % yield. The chemical identity of **TBP 1** was unambiguously confirmed by MALDI-TOF MS analysis in the solid state, as depicted in Figure S5. There is only one dominant peak in the respective mass spectra of **TBP 1**, revealing its defined molecular composition. The isotopic distribution pattern of the mass peak is in good agreement with the calculated one.

Then, **TBP 1** was further investigated by variable temperature  $^1\text{H}$  NMR spectra. A well-resolved  $^1\text{H}$  NMR spectrum in  $\text{CD}_2\text{Cl}_2$  solution was obtained at 213 K. The NMR peaks could be assigned to the structure of **TBP 1** with the help of 2D-COSY NMR spectroscopy (Figure S7). Interestingly, when the temperature was increased, the peaks became weaker and disappeared at room temperature. The  $^1\text{H}$  NMR spectra of the aromatic region of **TBP 1** are depicted in Figure 2. This process was reversible as cooling the sample back to 213 K gave the same spectrum (Figure S9). This result suggests a possible radical feature of **TBP 1** at room temperature. A similar phenomenon has been observed in phen-



Scheme 2. Synthetic route toward **TBP 1**.

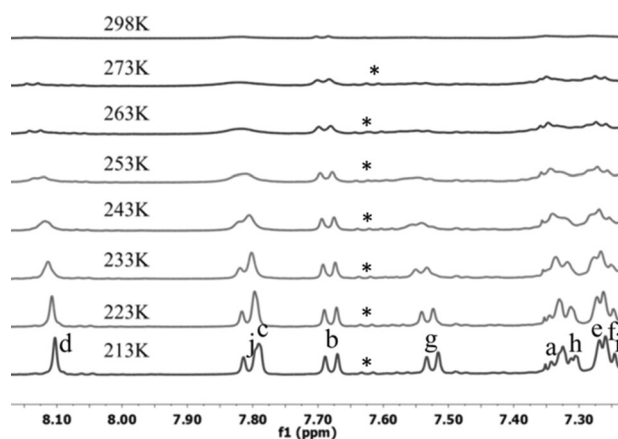


**Figure 2.** Variable-temperature  $^1\text{H}$  NMR spectra of **TBP 1** in  $\text{CD}_2\text{Cl}_2$  in the aromatic region.

lenyl-, zethrene-, and teranthene-based biradicals, resulting from a thermally excited triplet species which is slightly higher in energy than the singlet biradical state.<sup>[8,10,11]</sup>

Therefore, an electron paramagnetic resonance (EPR) measurement was carried out both in solution and the solid state to further confirm the biradical nature of **TBP 1** (Figure 3). A freshly prepared solution of **TBP 1** in toluene

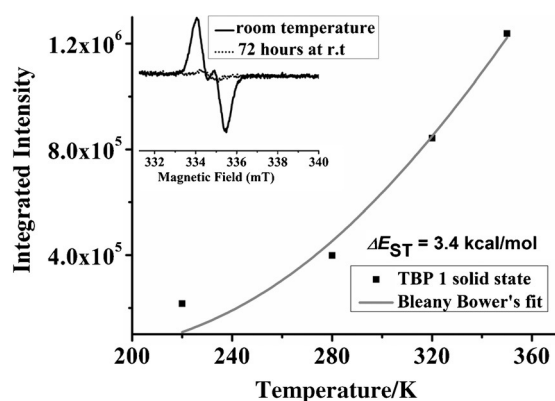


**Figure 3.** The change in EPR signal intensity with temperature (■) and the Bleaney–Bower's fit (—). Inset: EPR spectra of **TBP 1** in toluene solution at room temperature and after 72 h.

gave unresolved EPR spectra for a biradical with a broad peak at  $g$ -value 2.0035. At the center of the broad peak a tiny low intensity peak was also observed which was attributed to a monoradical impurity. The powder sample of **TBP 1** was also EPR-active indicating its biradical feature (Figure S16). Upon increasing the temperature, the EPR signal intensity increased which is in agreement with the variable temperature  $^1\text{H}$  NMR measurements. The Bleaney Bower's fit of the intensity change in EPR signals with temperature in the solid state gave a singlet-triplet energy gap of  $3.4 \text{ kcal mol}^{-1}$ . This phenomenon again supports the borderline character of **TBP 1** between a Kekulé structure and a biradical structure. Based on the NMR and EPR results we can safely conclude the biradical feature of compound **TBP 1**. The biradical structure of **TBP 1** can be described by three resonance forms,

**1-1**, **1-2**, and **1-3** (Figure 1). Whereas in **1-1** the two radical centers are protected by a bulky mesityl group, these two sites are unprotected in **1-2**. Thus, **TBP 1** was found to be unstable under ambient conditions. The time-dependent EPR measurement in toluene solution at room temperature indicated that the peak intensity decreased with the time, and that the signal almost disappeared after 72 h.

Next, the UV/Vis absorption of precursor **10** and **TBP 1** were characterized. The absorption spectra of **10** and **TBP 1** in dichloromethane (DCM) solution are compared in Figure 4a. Compound **10** exhibits a well-resolved absorption

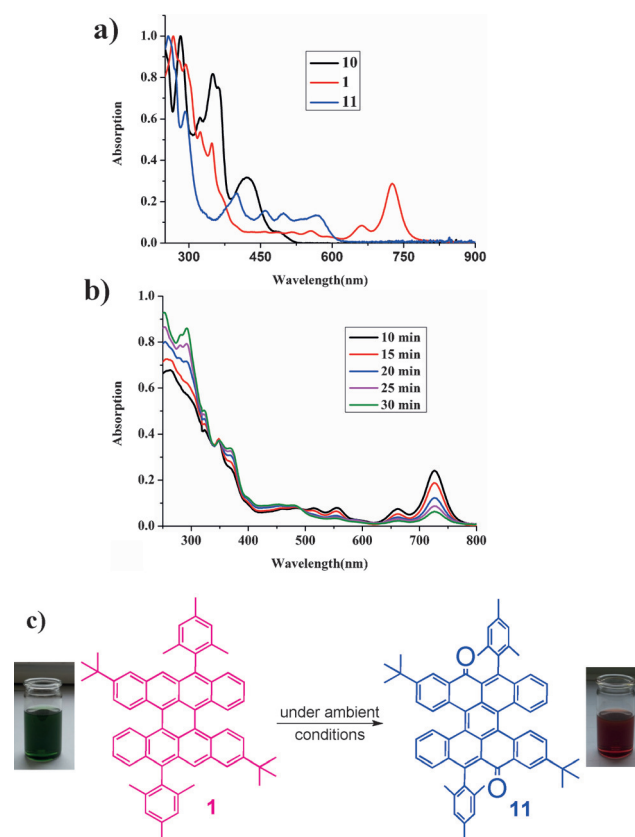


**Figure 4.** a) The UV/Vis spectra of the compounds **TBP 1**, **10**, and **11**. b) Time-dependent UV/Vis spectra of **TBP 1** at ambient conditions. c) Oxidation procedure from compound **TBP 1** to compound **11**.

maximum at 423 nm along with a small shoulder band peaking at 492 nm. Interestingly, the solution of **TBP 1** in DCM shows a green color and the absorption spectra yield a maximum in the near-infrared region (NIR) at 727 nm. Thus, a low optical energy gap of  $1.56 \text{ eV}$  for **TBP 1** is derived from the onsets of its UV/Vis absorption spectra. Moreover, **TBP 1** does not show any photoluminescence, which is a common behavior of biradicaloids.<sup>[10b,11c]</sup> This result again supports that both the Kekulé and biradical forms contribute similarly to the ground state.

Notably, the color of **TBP 1** changed quickly when exposed to air, suggesting that the oxidation took place at the zigzag edge of **TBP 1** as the reactive site. Thus, the time-dependent UV/Vis measurement was further performed under ambient conditions to examine the stability of **TBP 1**.

While the intensity of the absorption maximum in the NIR region (727 nm) decreased, the absorption peak at high energy (295 nm) increased with time (Figure 4b). The decay time ( $t$ ) was obtained from the least square fitting by using the following equations;<sup>[13]</sup>

$$A(t)/A(0) = \exp(-t/\tau) \quad (1)$$

$$A(t)/A(0) = \alpha \exp(-t/\tau_1) + (1-\alpha) \exp(-t/\tau_2) \quad (2)$$

in which  $A(t)$  is the absorbance of the low-energy  $\lambda_{\max}$  at time  $t$  and  $\tau$  is the lifetime,  $\alpha$  is the purity of the radical and the contribution of  $(1-\alpha)$  comes probably from the precursor. Then the calculated lifetime ( $\tau$ ) of **TBP 1** is approximately 35 min based on this equation. Finally, a red color was achieved for the oxidized product, which was identified as tetrabenzo[a,f,j,o]perylene-9,19-dione (**11**; Figure 4c), as confirmed by NMR spectroscopy and MALDI-TOF MS analysis (Figures S10–S13). The UV/Vis absorption of **11** is compared with **TBP 1** in Figure 4a. Apparently, compound **11** shows a significant blue shift (by 156 nm) for the visible-light absorption band relative to that of **TBP 1**, resulting in a relatively large optical energy gap of 2.04 eV compared to that of **TBP 1**.

To gain insight into the electronic structure of **TBP 1**, DFT calculations were conducted at the B3LYP/6-31G(d,p) level of theory using the Gaussian 09 program package. There are two stereoisomers of the compound **TBP 1**, for which *M*-**TBP-1** is more stable than *P*-**TBP-1** (Figure S22). The calculations show that the bistetracene **TBP 1** has a moderate singlet biradical character index ( $y = 0.615$ ), as calculated by using the occupation numbers of the spin-unrestricted Hartree–Fock natural orbitals. This result is in agreement with the above NMR and EPR analysis which demonstrates the biradicaloid nature of **TBP 1**. The SOMO  $\alpha$  and  $\beta$  orbitals and spin density are highly delocalized (Figure 5). Whereas the carbons C5 and C6 have the largest spin densities, the adjacent carbons C4 and C7 show much smaller spin densities (Figure 5b). These results indicate that the **TBP 1** should be described as a resonance form between the Kekulé and biradical structure shown in Figure 1. Furthermore, it was found that the energy of the singlet biradical state is lower than that of the triplet biradical and closed shell state (Table S1 in SI). From the calculation, the singlet-triplet energy gap ( $\Delta E_{S-T}$ ) is 6.7 kcal mol<sup>−1</sup>, meaning that **TBP 1** features a singlet biradical ground state. In addition, the harmonic oscillator model of aromaticity (HOMA)<sup>[14]</sup> values, which are geometry based aromaticity indices, indicates more benzenoid character for the peripheral and central six-membered rings (Figure S24). These findings strongly suggest that the formation of aromatic sextets overwhelms the penalty for breaking the  $\pi$ -bond and pushes the resulting unpaired electrons out to the zigzag edges.<sup>[10b]</sup>

In summary, we have synthesized the tetrabenzo-[a,f,j,o]perylene, namely “bistetracene” with two tetracenes connected side by side with two bonds. Such a zigzag-edged PAH exhibits a remarkable singlet biradical feature as proven by variable temperature <sup>1</sup>H NMR and EPR spectroscopy, which is well supported by DFT calculations. Such zigzag-

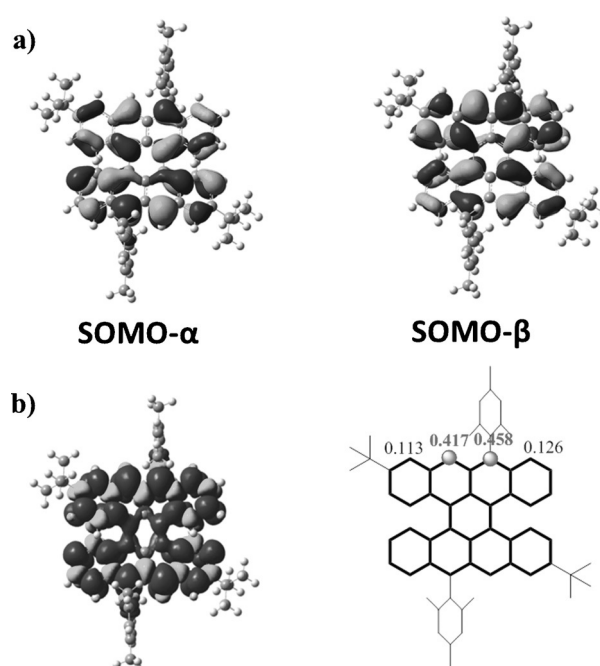


**Figure 5.** a) Calculated SOMOs for the  $\alpha$  and  $\beta$  electrons of the singlet biradical of **TBP 1**. b) The spin-density distribution of the triplet ground state of the bistetracene and the numbers given denote the spin density of the specific carbon atoms.

edged PAH can be considered as a short segment of infinite graphene nanoribbons with exceptionally long zigzag edges. Therefore, our studies contribute to an understanding of the edge states of expanded PAH homologues and graphene nanoribbons, which may possess a localized nonbonding  $\pi$ -state around the zigzag edges. It is envisioned that these zigzag-edged PAHs are promising candidates for the development of spintronics given that the edge-localized spins can be polarized by applying external magnetic/electrical fields.

**Keywords:** biradical · bistetracene · perylenes · polycyclic arenes · zigzag-edge

**How to cite:** *Angew. Chem. Int. Ed.* **2015**, *54*, 12442–12446  
*Angew. Chem.* **2015**, *127*, 12619–12623

- [1] a) J. E. Anthony, *Chem. Rev.* **2006**, *106*, 5028–5048; b) J. E. Anthony, *Angew. Chem. Int. Ed.* **2008**, *47*, 452–483; *Angew. Chem.* **2008**, *120*, 460–492; c) Q. Ye, C. Chi, *Chem. Mater.* **2014**, *26*, 4046–4056.
- [2] a) A. Hepp, H. Heil, W. Weise, M. Ahles, R. Schmechel, H. Seggern, *Phys. Rev. Lett.* **2003**, *91*, 157406; b) H. Moon, R. Zeis, E. J. Borkent, C. Besnard, A. J. Lovinger, T. Siegrist, C. Kloc, Z. Bao, *J. Am. Chem. Soc.* **2004**, *126*, 15322–15323; c) J. E. Anthony, J. S. Brooks, D. L. Eaton, S. R. Parkin, *J. Am. Chem. Soc.* **2001**, *123*, 9482–9483; d) Y. Diao, B. C. K. Tee, G. Giri, J. Xu, D. H. Kim, H. A. Becerril, R. M. Stoltenberg, T. H. Lee, G. Xue, S. C. B. Mannsfeld, Z. Bao, *Nat. Mater.* **2013**, *12*, 665–671; e) G. Giri, E. Verploegen, S. C. B. Mannsfeld, S. Atahan-Evrenk, D. H. Kim, S. Y. Lee, H. A. Becerril, A. Aspuru-Guzik, M. F. Toney, Z. Bao, *Nature* **2011**, *480*, 504–508.
- [3] a) B. Purushothaman, M. Bruzek, S. R. Parkin, A. F. Miller, J. E. Anthony, *Angew. Chem. Int. Ed.* **2011**, *50*, 7013–7017; *Angew. Chem.* **2011**, *123*, 7151–7155; b) C. Tönshoff, H. F. Bettinger,



- Angew. Chem. Int. Ed.* **2010**, *49*, 4125–4128; *Angew. Chem.* **2010**, *122*, 4219–4222.
- [4] a) D. E. Jiang, S. Dai, *Chem. Phys. Lett.* **2008**, *466*, 72–75; b) F. Moscardó, E. San-Fabián, *Chem. Phys. Lett.* **2009**, *480*, 26–30.
- [5] a) L. B. Roberson, J. Kowalik, L. M. Tolbert, C. Kloc, R. Zeis, X. L. Chi, R. Fleming, C. Wilkins, *J. Am. Chem. Soc.* **2005**, *127*, 3069–3075; b) B. H. Northrop, J. E. Norton, K. N. Houk, *J. Am. Chem. Soc.* **2007**, *129*, 6536–6546.
- [6] a) Z. Sun, J. Wu, *J. Mater. Chem.* **2012**, *22*, 4151–4160; b) Z. Sun, Q. Ye, C. Chi, J. Wu, *Chem. Soc. Rev.* **2012**, *41*, 7857–7889; c) J. Li, K. Zhang, X. Zhang, K. Huang, C. Chi, J. Wu, *J. Org. Chem.* **2010**, *75*, 856–863; d) E. H. Fort, P. M. Donovan, L. T. Scott, *J. Am. Chem. Soc.* **2009**, *131*, 16006–16007.
- [7] a) Z. Sun, Z. Zeng, J. Wu, *Acc. Chem. Res.* **2014**, *47*, 2582–2591; b) Z. Sun, Z. Zeng, J. Wu, *Chem. Asian J.* **2013**, *8*, 2894–2904; c) A. Shimizu, M. Nakanob, Y. Hirao, T. Kubo, *J. Phys. Org. Chem.* **2011**, *24*, 876–882; d) T. Kubo, *Chem. Rec.* **2014**, DOI: 10.1002/tcr.201402065.
- [8] a) K. Ohashi, T. Kubo, T. Masui, K. Yamamoto, K. Nakasuji, T. Takui, Y. Kai, I. Murata, *J. Am. Chem. Soc.* **1998**, *120*, 2018–2027; b) T. Kubo, M. Sakamoto, M. Akabane, Y. Fujiwara, K. Yamamoto, M. Akita, K. Inoue, T. Takui, K. Nakasuji, *Angew. Chem. Int. Ed.* **2004**, *43*, 6474–6479; *Angew. Chem.* **2004**, *116*, 6636–6641; c) T. Kubo, A. Shimizu, M. Sakamoto, M. Uruichi, K. Yakushi, M. Nakano, D. Shiomi, K. Sato, T. Takui, Y. Morita, K. Nakasuji, *Angew. Chem. Int. Ed.* **2005**, *44*, 6564–6568; *Angew. Chem.* **2005**, *117*, 6722–6726; d) A. Shimizu, M. Uruichi, K. Yakushi, H. Matsuzaki, H. Okamoto, M. Nakano, Y. Hirao, K. Matsumoto, H. Kurata, T. Kubo, *Angew. Chem. Int. Ed.* **2009**, *48*, 5482–5486; *Angew. Chem.* **2009**, *121*, 5590–5594; e) A. Shimizu, Y. Hirao, K. Matsumoto, H. Kurata, T. Kubo, M. Uruichi, K. Yakushi, *Chem. Commun.* **2012**, *48*, 5629–5631; f) K. Uchida, Y. Hirao, H. Kurata, T. Kubo, S. Hatano, K. Inoue, *Chem. Asian J.* **2014**, *9*, 1823–1829; g) P. Ravat, M. Baumgarten, *Phys. Chem. Chem. Phys.* **2015**, *17*, 983–991.
- [9] a) A. Le Berre, *Ann. Chim.* **1957**, *13*, 371–425; b) D. T. Chase, A. G. Fix, B. D. Rose, C. D. Weber, S. Nobusue, C. E. Stockwell, L. N. Zakharov, M. C. Loneragan, M. M. Haley, *Angew. Chem. Int. Ed.* **2011**, *50*, 11103–11106; *Angew. Chem.* **2011**, *123*, 11299–11302; c) D. T. Chase, B. D. Rose, S. P. McClintock, L. N. Zakharov, M. M. Haley, *Angew. Chem. Int. Ed.* **2011**, *50*, 1127–1130; *Angew. Chem.* **2011**, *123*, 1159–1162; d) D. T. Chase, A. G. Fix, S. J. Kang, B. D. Rose, C. D. Weber, Y. Zhong, L. N. Zakharov, M. C. Loneragan, C. Nuckolls, M. M. Haley, *J. Am. Chem. Soc.* **2012**, *134*, 10349–10352; e) A. Shimizu, Y. Tobe, *Angew. Chem. Int. Ed.* **2011**, *50*, 6906–6910; *Angew. Chem.* **2011**, *123*, 7038–7042; f) A. Shimizu, R. Kishi, M. Nakano, D. Shiomi, K. Sato, T. Takui, I. Hisaki, M. Miyata, Y. Tobe, *Angew. Chem. Int. Ed.* **2013**, *52*, 6076–6079; *Angew. Chem.* **2013**, *125*, 6192–6195.
- [10] a) A. Konishi, Y. Hirao, M. Nakano, A. Shimizu, E. Botek, B. Champagne, D. Shiomi, K. Sato, T. Takui, K. Matsumoto, H. Kurata, T. Kubo, *J. Am. Chem. Soc.* **2010**, *132*, 11021–11023; b) A. Konishi, Y. Hirao, K. Matsumoto, H. Kurata, R. Kishi, Y. Shigeta, M. Nakano, K. Tokunaga, K. Kamada, T. Kubo, *J. Am. Chem. Soc.* **2013**, *135*, 1430–1437.
- [11] a) Z. Sun, K. W. Huang, J. Wu, *J. Am. Chem. Soc.* **2011**, *133*, 11896–11899; b) Y. Li, W. K. Heng, B. S. Lee, N. Aratani, J. L. Zafra, N. Bao, R. Lee, Y. M. Sung, Z. Sun, K. W. Huang, R. D. Webster, J. T. L. Navarrete, D. Kim, A. Osuka, J. Casado, J. Ding, J. Wu, *J. Am. Chem. Soc.* **2012**, *134*, 14913–14922; c) Z. Sun, S. Lee, K. H. Park, X. Zhu, W. Zhang, B. Zheng, P. Hu, Z. Zeng, S. Das, Y. Li, C. Chi, R. W. Li, K. W. Huang, J. Ding, D. Kim, J. Wu, *J. Am. Chem. Soc.* **2013**, *135*, 18229–18236; d) S. Das, S. Lee, M. Son, X. Zhu, W. Zhang, B. Zheng, P. Hu, Z. Zeng, Z. Sun, W. Zeng, R. W. Li, K. W. Huang, J. Ding, D. Kim, J. Wu, *Chem. Eur. J.* **2014**, *20*, 11410–11420; e) Y. Li, K. W. Huang, Z. Sun, R. D. Webster, Z. Zeng, W. Zeng, C. Chi, K. Furukawa, J. Wu, *Chem. Sci.* **2014**, *5*, 1908–1914.
- [12] E. Clar, *The Aromatic Sextet*, Wiley, London, **1972**.
- [13] Y. Kawanaka, A. Shimizu, T. Shinada, R. Tanaka, Y. Teki, *Angew. Chem. Int. Ed.* **2013**, *52*, 6643–6647; *Angew. Chem.* **2013**, *125*, 6775–6779.
- [14] a) J. Kruszewski, T. M. Krygowski, *Tetrahedron Lett.* **1972**, *13*, 3839–3842; b) T. M. Krygowski, *J. Chem. Inf. Comput. Sci.* **1993**, *33*, 70–78.

Received: March 23, 2015

Published online: June 12, 2015